particles

MDPI

Article

Stability of Spherical Nuclei in the Inner Crust of Neutron Stars

Nikita A. Zemlyakov [1,2,*] and Andrey I. Chugunov [1]

[1] Ioffe Institute, 26 Politekhnicheskaya st., St. Petersburg 194021, Russia; andr.astro@mail.ioffe.ru
[2] Institute of Physics and Mechanics, Peter the Great St. Petersburg Polytechnic University, 29 Politekhnicheskaya st., St. Petersburg 195251, Russia
* Correspondence: zemnic5@gmail.com

Abstract: Neutron stars are the densest objects in the Universe. In this paper, we consider the so-called inner crust—the layer where neutron-excess nuclei are immersed in the degenerate gas of electrons and a sea of quasi-free neutrons. It was generally believed that spherical nuclei become unstable with respect to quadrupole deformations at high densities, and here, we consider this instability. Within the perturbative approach, we show that spherical nuclei with equilibrium number density are, in fact, stable with respect to infinitesimal quadrupole deformation. This is due to the background of degenerate electrons and associated electrostatic potential, which maintain stability of spherical nuclei. However, if the number of atomic nuclei per unit volume is much less than the equilibrium value, instability can arise. To avoid confusion, we stress that our results are limited to infinitesimal deformations and do not guarantee strict thermodynamic stability of spherical nuclei. In particular, they do not exclude that substantially non-spherical nuclei (so-called pasta phase) represent a thermodynamic equilibrium state of the densest layers of the neutron star crust. Rather, our results point out that spherical nuclei can be metastable even if they are not energetically favourable, and the timescale of transformation of spherical nuclei to the pasta phases should be estimated subsequently.

Keywords: neutron stars; dense matter; Bohr–Wheeler criteria; stability of spherical nuclei; inner crust

Citation: Zemlyakov, N.A.; Chugunov, A.I. Stability of Spherical Nuclei in the Inner Crust of Neutron Stars. *Particles* **2022**, *5*, 225–234. https://doi.org/10.3390/particles5030020

Academic Editor: Armen Sedrakian

Received: 27 May 2022
Accepted: 29 June 2022
Published: 1 July 2022

1. Introduction

The inner crust of neutron stars extends from the density $\rho_{\rm drip} \approx 4.3 \times 10^{11}$ g/cm^3 to $\sim 10^{14}$ g/cm^3 [1,2]. It consists of fully ionised atomic nuclei immersed in a background of quasi-free neutrons and relativistic degenerate electron gas. Atomic nuclei have large neutron excess because of the high chemical potential of the electrons. They have a spherical shape in most of the inner crust, but in the deepest layers, energetically favourable nuclei configurations can become substantially non-spherical (cylinders, planes and inverse configurations; so-called pasta phases) [1–6] (see also [7–10] for the most recent progress). Note, however, that some works (e.g., [11,12]) predict pasta phases to be absent in neutron stars.

Following [13], the density region for spherical nuclei was generally assumed to be limited by instability of spherical nuclei with respect to quadrupole deformations (see, e.g., [1,2,14]). Namely, applying the instability criterion derived by Bohr and Wheeler [15] for an isolated nucleus, the spherical nuclei were predicted to become absolutely unstable (even for infinitesimal deformation) when the ratio of the nucleus volume to the Wigner–Seitz cell volume (filling factor) u reaches a value of $1/8 = 0.125$ [13]. Indeed, recently the extended Thomas–Fermi calculations of Ref. [8] report a transition from spherical to cylindrical nuclei at a filling factor close to 0.125 (see their Table XII and respective discussion). However, calculations within the compressible liquid drop model (CLDM) typically predict spherical nuclei to be energetically favourable up to the larger filling factor $\sim$0.2 (see, e.g., [4,11] and Figure 1 for numerical illustration). Thus, at least within the CLDM approach, there is a contradiction between numerical results and predicted instability: spherical nuclei are predicted to be thermodynamically stable at the region where they are supposed to be

absolutely unstable. Obviously, we have two (not mutually exclusive) solutions: (A) the true thermodynamic equilibrium for filling factors 0.125–0.2 correspond to complex nuclear structures (e.g., [9]), which stays beyond the scope of most works based on the CLDM approach; (B) the instability of spherical nuclei is suppressed in the inner crust.

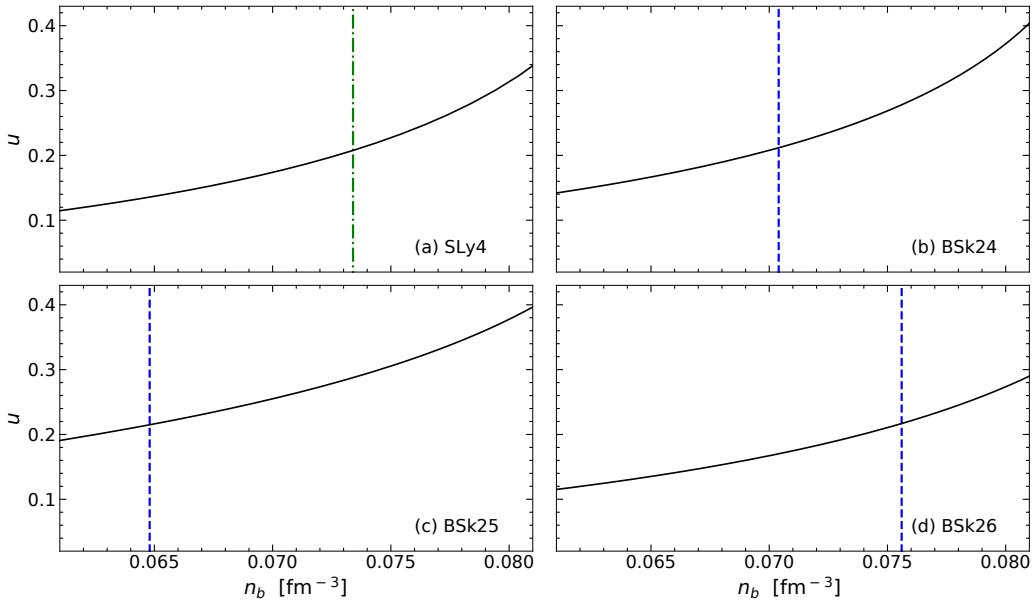

Figure 1. The filling factor for spherical nuclei as a function of nucleon number density. Panels (**a**–**d**) are plotted for the Skyrme potentials SLy4 [16,17] and BSk24, BSk25, BSk26 [18], respectively. The black solid line is the filling factor, the vertical lines represent maximal density of the spherical nuclei predicted to be energetically favourable. For the SLy4 model (panel **a**, dash-dot line) it corresponds to the transition from spherical to the uniform nuclear matter (neutron star core), while for BSk models (panels **b**–**d**; dashed line), the transition to the cylindrical nuclei takes place. The plot is based on calculations of Ref. [19].

For option (B), enhanced stability of spherical nuclei were suggested by a number of authors (e.g., [11,20]). The strongest point in support of this solution was suggested in Ref. [21], which, in particular, investigated the stability of spherical nuclei with respect to infinitesimal deformations within the Wigner–Seitz cell approximation. Authors concluded that spherical nuclei are stable at an arbitrary filling factor, if the number density of nuclei corresponds to the optimal value. (The so-called virial theorem, derived by [22] and applied by authors of Ref. [21] (see Equation (2) here), is applicable only for the optimal number density of nuclei.) However, in our opinion, results of Ref. [21] are based on inaccurate boundary conditions. Namely, to ensure that the electric field flux over the cell boundary is zero, authors of Ref. [21] impose the Nuemann boundary condition, i.e., demand that the normal component of the electric field is zero at each point of the cell boundary. The latter seems unreasonable: thanks to the zero charge of the cell and Gauss theorem, the electric field flux over the cell boundary vanishes automatically if electron and nucleus (proton) contributions are both correctly incorporated. Imposing of specific boundary conditions, in particular, the Neumann boundary condition, is equal to the assumption that the charges outside the cell rearrange themselves to a distribution, which is required to ensure the imposed boundary condition. Note, that the required distribution of outside charges depends on deformation of the nucleus, making such rearranging unnatural from our point of view. Here, we correct this problem. In addition, our consideration naturally takes into account the neutron skin, which is an essential ingredient of two-phase system boundary thermodynamics (e.g., [23,24]), however, accounting for this effect does not change the results.

Note, according to [13], the corrections to Bohr and Wheeler [15] instability conditions associated with the presence of other nuclei and electrons were already calculated by Brandt [25]. However, the latter work is unavailable for us and authors of [13] neglect these corrections.

To avoid confusion, let us stress that we analyse only stability with respect to infinitesimal deformations. Clearly, it is not sufficient to guarantee absolute thermodynamic stability. Indeed, as shown by Hashimoto et al. [4], the spherical nuclei can not be energetically favourable at too large filling factors, and thus spherical nuclei, can be treated only as metastable in a strict thermodynamic sense.

2. Calculations

In order to explain the nature of the above mentioned contradictions, we checked the validity of option B): suppression of spherical nuclei instability in the inner crust. We applied the CLDM of Ref. [26], in which the nucleus is surrounded by quasi-free neutrons, being located at the center of a spherical Wigner–Seitz cell, which is uniformly filled with electrons (according to the quasi-neutrality requirement the total charge of the cell is zero). This model naturally incorporates neutron skin effects (see supplementary material to Ref. [26] for details).

Following Bohr and Wheeler [15], we considered the change of energy when the nucleus is deformed from a sphere to a spheroid with semi-axes $R(1+\varepsilon)$ and $R/\sqrt{1+\varepsilon}$. Here, R is the radius of the spherical nucleus, ε is an infinitesimal deformation parameter. The Wigner–Seitz cell is assumed to stay spherical. Within the CLDM of Ref. [26], the change of the cell energy can be calculated analytically up to the second order in ε (see Appendix A for the details):

$$\delta E = \left[\frac{8\pi R^2}{5}\sigma + \frac{3}{5}\left(\frac{u}{2} - \frac{1}{5}\right)\frac{Z^2e^2}{R}\right]\varepsilon^2, \tag{1}$$

where, σ is the surface tension, R is the radius of the nucleus before deformation, Ze is the nucleus charge, e is the elementary charge. Equation (1) is similar to Equation (9) of Ref. [15], but does not coincide exactly (even for ε^2 terms, considered here) due to the presence of electron background, which induces electrostatic potential and modifies the Coulomb energy change associated with nuclei deformation. The difference is $\propto u$. It agrees with the results of Ref. [25], as they were cited in [13]. However, as we demonstrate below, this term can not be neglected because it leads to suppression of the instability.

It is worth stressing that Equation (1) holds true in exactly the same form for a simplified CLDM, which neglects neutron skin effects (see Appendix A.2 for derivation details), so our results are equally applicable for this widely applied type of CLDM.

2.1. Equilibrium Inner Crust

The virial theorem [22] (see also supplementary material in [26] for derivation with accurate account of neutron adsorption effects) provides coupling for Coulomb energy and surface terms, if crust composition corresponds to the equilibrium (the number of atomic nuclei per unit volume is optimal):

$$4\pi\sigma R^2 = 2\frac{3}{5}\frac{Z^2e^2}{R}\left(1 - \frac{3}{2}u^{\frac{1}{3}} + \frac{1}{2}u\right). \tag{2}$$

Substituting $4\pi\sigma R^2$, given by (2), into Equation (1), we got the energy change associated with infinitesimal nuclei deformation in the equilibrium crust:

$$\delta E = \frac{3}{5}\frac{Z^2e^2}{R}\left(\frac{3}{5} - \frac{6}{5}u^{\frac{1}{3}} + \frac{9}{10}u\right)\varepsilon^2. \tag{3}$$

It is easy to check that at any value of the filling factor $u \in (0,1)$, the energy change δE, remains positive. Thus, the nuclei in the crust with equilibrium composition remain stable with respect to infinitesimal quadrupole deformations at any values of the filling factor. It is worth stressing that this result is derived analytically and stays the same for CLDMs, which includes and neglects neutron skin effects. In particular, it does not depend on the choice of nuclear physical model required to specify numerical parameters of CLDM (e.g., the bulk energy and surface tension). Note that the equilibrium composition is believed to be a good model for nonaccreting neutron stars [1] (see, however, [27,28]).

2.2. Non-Equilibrium Inner Crust

In the more general case, the number of atomic nuclei per unit volume can differ from the equilibrium value. In this case, instead of (2), we can write the more general expression [26]:

$$4\pi\sigma R^2 - 2\frac{3}{5}\frac{Z^2e^2}{R}\left(1 - \frac{3}{2}u^{\frac{1}{3}} + \frac{1}{2}u\right) = 3\mu_N. \tag{4}$$

where μ_N is the the chemical potential of the nucleus, which describes the change in energy when one nucleus is created from nucleons, which are already present in the substance (for equilibrium crust $\mu_N = 0$).

Combining Equations (1) and (4), we obtain the energy change associated with the deformation of a nucleus in the non-equilibrium crust:

$$\delta E = \frac{3}{5}\frac{Z^2e^2}{R}\left(\frac{3}{5} - \frac{6}{5}u^{\frac{1}{3}} + \frac{9}{10}u\right)\varepsilon^2 + \frac{6}{5}\mu_N\varepsilon^2. \tag{5}$$

For accreting neutron stars, there is an excess of nuclei in the crust [26]. It leads to $\mu_N > 0$ and makes the spherical nuclei even more stable with respect to quadrupole deformations. (To avoid confusion, let us point out that the instability considered in [26] is not associated with deformation of nuclei and this study does not alter any results of [26]) If $\mu_N < 0$, i.e., when the number density of nuclei in the stellar matter is less than the equilibrium value, the nuclei may become unstable with respect to quadrupole deformations and this instability likely leads to fission.

For numerical illustration of possible instability, we perform calculations, including neutron skin (adsorption) effects within the CLDM of Ref. [26] and apply the SLy4 nucleon–nucleon potential [16,17]. We parametrize matter by baryon number density n_b and parameter $C = \mu_N/\mu_n$, which stays constant in the inner crust thanks to diffusion/hydrostatic equilibrium of quasi-free neutrons [26]. The results are shown in Figure 2 for several values of C.

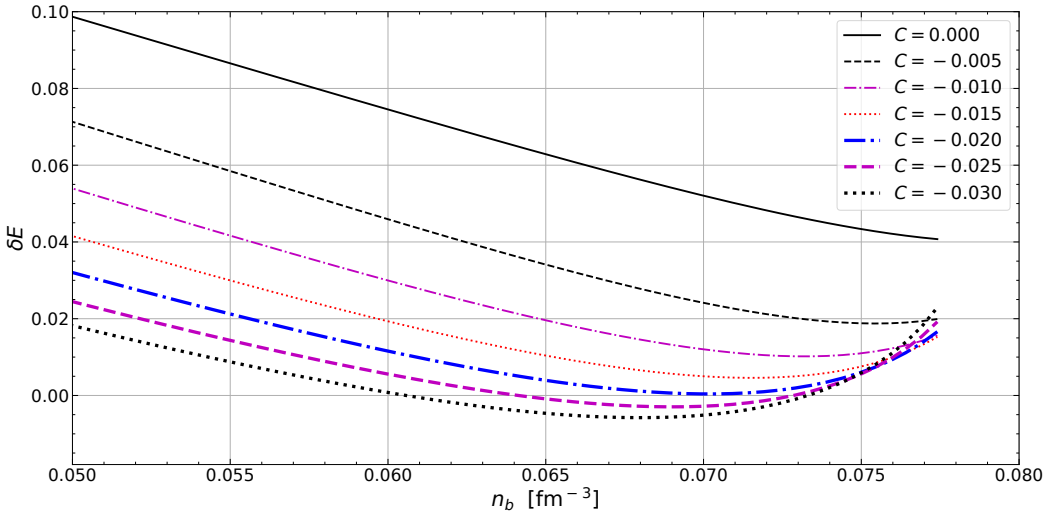

Figure 2. δE normalized to $Z^2e^2\varepsilon^2/R$ as a function of nucleon number density for different values of $C = \mu_N/\mu_n$. The neutron skin effects are included within CLDM of Ref. [26]. SLy4 potential [16,17] is applied.

3. Discussion, Results and Conclusions

Within CLDM we demonstrate that spherical nuclei are stable with respect to infinitesimal quadrupole deformations, if their number density correspond to the equilibrium value. The suppression of the instability, in comparison with isolated nuclei, is due to the fact that nuclei in the inner crust are immersed into a background of degenerate electrons. The electron charge density is comparable with the charge density of the nucleus and induces electrostatic potential, which supports the spherical shape of nuclei.

For a non-equilibrium crust, when the number of nuclei per unit volume is less than the equilibrium number, the instability with respect to infinitesimal quadrupole deformations can appear. This results seems natural: fission, likely caused by instability, leads to an increase in the nuclei number, driving the composition closer to the equilibrium. According to our calculations for SLy4 potential [16,17], nuclei number density should be lower than the equilibrium value by a factor of 2.2–2.4 to ensure the instability at $n_b > 0.047$ fm^{-3}. If nuclei number density is larger than the equilibrium at the same baryon density (e.g., in the accreted crust [26]), the spherical nuclei are stable with respect to an infinitesimal deformation. However, it does not exclude other types of instability which are not associated with nuclei deformation, for example, the instability considered in [26].

Qualitatively similar results were obtained in [21], but as we point out in the Introduction, this work appeals to artificial boundary conditions. It leads to quantitative differences with our results.

It is worth stressing that our analysis is perturbative, and thus limited to infinitesimal deformations. Obviously, it can not guarantee absolute thermodynamic stability of spherical nuclei. Indeed, the cylindrical and other pasta phases are shown to become more energetically favourable at large filling factors, $u \gtrsim 0.2$ [4]. Combination of stability of spherical nuclei for infinitesimal deformations with instability in a strict thermodynamic sense for $u \gtrsim 0.2$ suggests that in this conditions spherical nuclei should be, in fact, metastable (i.e., correspond to local energy minimum, which differs from the global minimum). It opens an interesting task to estimate the transition timescale from spherical to nonspherical shapes, however, we leave any estimates for this timescale beyond this work. However, we point out that the $u = 1/8$ criterion should not be applied to an upper bound for the density region of spherical nuclei in equilibrium crust because it was suggested on the basis of a simplified consideration of the fission instability, which is not supported by more detailed analyses, as in our work.

Concluding, we should warn the reader than all our results are obtained within spherical Wigner–Seitz cell approximation, which is likely inaccurate and should be elaborated for very large filling factor $u \sim 1$. However, in realistic models of crust, the filling factor for spherical nuclei is $u \lesssim 0.2$ and the spherical Wigner–Seitz cell seems a reasonable approximation, but we do not check the latter statement straightforwardly. We also warn that we neglect the curvature corrections to the surface tension, which are shown to be important for thermodynamically determined boundaries of the pasta layers (e.g., [29]), however, we do not expect that it can affect our results qualitatively.

Author Contributions: Derivations, figures and original draft preparation N.A.Z.; formulation of the problem, final edition of the draft and supervision A.I.C. All authors have read and agreed to the published version of the manuscript.

Funding: Work of N.A.Z. was funded was funded by the Russian Science Foundation grant number 19-12-00133-P. https://rscf.ru/project/19-12-00133/, (accessed on 30 June 2022).

Data Availability Statement: Not applicable.

Conflicts of Interest: The authors declare no conflict of interest. The funders had no role in the design of the study; in the collection, analyses or interpretation of data; in the writing of the manuscript, or in the decision to publish the results.

Abbreviations

The following abbreviations are used in this manuscript:

CLDM	Compressible liquid drop model
SLy	Skyrme–Lyon
BSk	Brussels–Skyrme

Appendix A. Derivation of the Energy Change Associated with Nuclei Deformation

In this appendix we derive Equation (1), which describes the change of the cell energy associated with nuclei deformation. The derivations are provided for two versions of CLDM, one which neglects neutron skin effects and the model of Ref. [26], which incorporates these effects thermodynamically consistently. The curvature corrections are neglected in both cases. In the first Appendix A.1, we derive the Coulomb energy of a cell with deformed nuclei, which is required for derivation of Equation (1).

Appendix A.1. Coulomb Energy of the Cell with Deformed Nucleus

We start from consideration of the Coulomb energy of a cell with deformed nucleus in the center. It is essentially an electrostatic problem: calculation of the Coulomb energy of a uniformly negatively charged sphere with radius $R_c = R/u^{1/3}$ and uniformly positively charged spheroid (with semi-axes $R(1+\varepsilon)$ and $R/\sqrt{1+\varepsilon}$), located at the center of the sphere. The net charge of this system is zero. We neglect terms $\propto \varepsilon^3$.

We begin with the Poisson's equation for the Wigner–Seitz cell:

$$\Delta\varphi = -4\pi\left[\rho_p\Theta(R_{sp}(\theta) - r) + \rho_e\Theta\left(\frac{R}{u^{1/3}} - r\right)\right], \tag{A1}$$

where r and θ are the radial distance and the polar angle of the spherical coordinate system ($r = 0$ is the center of the cell), $\Theta(x)$ is the Heaviside step function. $\rho_{pi} = Ze/(4\pi R^3/3)$ is the proton charge density inside nucleus, $\rho_e = -u\rho_{pi}$ is the electron charge density (the cell is electrically neutral). The protons are located within a spheroid, with boundary given by:

$$R_{sp}(\theta) = \frac{R}{\sqrt{(1 - cos^2\theta)(1+\varepsilon) + cos^2\theta/(1+\varepsilon)^2}}. \tag{A2}$$

It is worth stressing, that ρ_p does not depend on ε because we consider the deformation which does not affect nucleus volume.

The solution to Equation (A1) can be presented as a sum of the proton potential φ_p and the electron potential φ_e, while the total Coulomb energy can be presented as $E_C = E_C^{p-p} + E_C^{e-p} + E_C^{e-e}$, where terms E_C^{p-p}, E_C^{e-p}, and E_C^{e-e} are proton-proton, electron-proton, and electron-electron contributions, respectively:

$$E_C^{p-p} = \frac{1}{2}\int \rho_p(\boldsymbol{r})\varphi_p(\boldsymbol{r})d^3\boldsymbol{r} = \frac{1}{2}\int_{r<R_{sp}(\theta)} \rho_p\varphi_p(\boldsymbol{r})d^3\boldsymbol{r}, \tag{A3}$$

$$E_C^{e-p} = \int \rho_p(\boldsymbol{r})\varphi_e(\boldsymbol{r})d^3\boldsymbol{r} = \int_{r<R_{sp}(\theta)} \rho_p\varphi_e(\boldsymbol{r})d^3\boldsymbol{r}, \tag{A4}$$

$$E_C^{e-e} = \frac{1}{2}\int \rho_e(\boldsymbol{r})\varphi_e(\boldsymbol{r})d^3\boldsymbol{r} = \frac{1}{2}\int_{r<R_c} \rho_e\varphi_e(\boldsymbol{r})d^3\boldsymbol{r}. \tag{A5}$$

Here, we take into account that proton density is zero outside the spheroid.

The explicit form of electron potential inside the cell is:

$$\varphi_e = \frac{2\pi\rho_e R^2}{u^{2/3}} - \frac{2}{3}\pi\rho_e r^2, \tag{A6}$$

while the proton potential inside the nucleus ($r < R_{sp}(\theta)$) can be written in the form:

$$\varphi_p = 2\pi\rho_p R^2 - \frac{2}{3}\pi\rho_p r^2 + \frac{4}{5}\pi\rho_p r^2\varepsilon\left(\frac{3}{2}cos^2\theta - \frac{1}{2}\right) - \frac{2}{5}\pi\rho_p R^2\varepsilon^2 + \ldots, \tag{A7}$$

The omitted terms contributes to the Coulomb energy only at order ε^3 or higher, which is not considered here. The proton potential outside the nucleus is not required to calculate Coulomb energy (see Equations (A3)–(A5)) and thus not shown here.

The integrals in Equations (A3)–(A5) can be calculated analytically. Up to the second order in ε they are:

$$E_C^{p-p} = \frac{3}{5}\frac{(Ze)^2}{R} - \frac{3}{25}\frac{(Ze)^2}{R}\varepsilon^2, \tag{A8}$$

$$E_C^{e-p} = -\frac{3}{2}\frac{(Ze)^2}{R}u^{1/3} + \frac{3}{10}\frac{(Ze)^2}{R}u\left(1+\varepsilon^2\right), \tag{A9}$$

$$E_C^{e-e} = \frac{3}{5}\frac{(Ze)^2}{R}u^{1/3}. \tag{A10}$$

For $\varepsilon = 0$ they agree with the well-known expression for the Coulomb energy of the cell with spherical nucleus (e.g., [22]).

Appendix A.2. Calculation of the Energy Change Neglecting Neutron Skin

Within CLDM, which neglects the neutron skin, the surface tension is typically assumed to be function of x_i—the ratio of proton number density to the total baryon number density inside the nucleus. To derive Equation (1), we consider differences of the cell energies between two configurations: (a) WS cell with spherical nucleus and (b) WS cell with deformed nucleus. We assume that the proton and neutron number densities inside the nuclei as well as the neutron number density outside the nucleus are the same in both configurations. The volume of the nucleus is also unmodified by deformation. In this case, the energy change associated with deformation, $\delta E = E_b - E_a$, contain only surface and Coulomb terms, while the bulk terms cancel out.

The surface tension is the same in both configurations (x_i is not modified) and the surface energy change is given by the difference between the surface areas of the spheroid and the sphere. Thus, a change of the surface energy is:

$$\delta E_s = \frac{8}{5}\pi\sigma R^2\varepsilon^2. \tag{A11}$$

The change of the Coulomb energy can be calculated using the results of Appendix A.1, which leads to:

$$\delta E_C = \frac{3}{5}\frac{(Ze)^2}{R}\left(\frac{u}{2}-\frac{1}{5}\right)\varepsilon^2. \tag{A12}$$

The net energy change $\delta E = \delta E_C + \delta E_s$, thus summing up Equations (A11) and (A12), we obtain Equation (1).

Appendix A.3. Calculation of the Energy Change Including Neutron Skin

The derivation of Equation (1) for the CLDM of Ref. [26], which accounts for neutron skin (adsorption) effects, is more complicated. It is due to the nuclei deformation changes of nuclei surface area and the amount of neutrons adsorbed on it. Thus, one can not assume that neutron number densities and nucleus volume are not modified by deformation because it will lead to variation of the total number of neutrons (and thus the net baryon density).

To derive Equation (1), we consider an extended version CLDM of Ref. [26], which is allowed for deformed nuclei. Namely, the nucleus deformation parameter ε is added as an additional independent CLDM variable. It allows one to write down the expression for the energy density ϵ, which differs from Equation (2) of the supplementary material to Ref. [26], only by the Coulomb and surface energy terms:

$$\epsilon = u\,\epsilon^{\rm bulk}(n_{ni}, n_{pi}) + (1-u)\,\epsilon^{\rm bulk}(n_{no}, 0) + \frac{E_s(\nu_s, R, \varepsilon)}{V_c} + \frac{E_C(n_{pi}, R, u, \varepsilon)}{V_c} + e_e(n_e). \tag{A13}$$

where $\epsilon^{\rm bulk}(n_n, n_p)$ is the energy density of bulk nuclear matter at the respective neutron and proton number density (n_n and n_p), n_{ni}, n_{pi} are the neutron and proton number density inside the nucleus, n_{no} is the neutron number density outside the nucleus (we assume that proton drip does not take place), and $e_e(n_e)$ is the energy density of degenerate electrons at electron number density $n_e = u\,n_{pi}$. The cell volume $V_c = 4\pi R^3/(3u)$. According to the results of Appendix A.1, the Coulomb energy is:

$$E_C = \frac{3}{5}\frac{Z^2e^2}{R}\left[f(u) + \left(\frac{u}{2}-\frac{1}{5}\right)\varepsilon^2\right] = \frac{16\pi^2}{15}(n_{pi}e)^2R^5\left[f(u) + \left(\frac{u}{2}-\frac{1}{5}\right)\varepsilon^2\right], \tag{A14}$$

where $f(u) = 1 - 3\,u^{1/3}/2 + u/2$. The surface energy:

$$E_s = \mathcal{A}(\mu_{ns}\nu_s + \sigma), \tag{A15}$$

where μ_{ns} and ν_s are chemical potential and surface density of the adsorbed neutrons. The nuclei surface area $\mathcal{A}$ is given by the surface area of the spheroid:

$$\mathcal{A} = 4\pi R^2 + \frac{8}{5}\pi R^2\varepsilon^2. \tag{A16}$$

The thermodynamic consistency requires:

$$\frac{d\sigma}{d\nu_s} = -\nu_s\frac{d\mu_{ns}}{d\nu_s}. \tag{A17}$$

Thus, σ and μ_{ns} can be treated as functions of ν_s.

Following [26], let us introduce auxiliary variables, which simplifies the subsequent analysis:

$$n_{ni}^{(\mathrm{tot})} \equiv n_{ni}u, \tag{A18}$$
$$n_{pi}^{(\mathrm{tot})} \equiv n_{pi}u, \tag{A19}$$
$$n_{no}^{(\mathrm{tot})} \equiv n_{no}(1-u), \tag{A20}$$
$$n_{ns}^{(\mathrm{tot})} \equiv \frac{N_s}{V_c}, \tag{A21}$$
$$n_N = V_c^{-1}. \tag{A22}$$

where $N_s = \mathcal{A}\nu_s$ is the number of neutrons adsorbed to the nucleus.

Here, we analyse stability with respect to an infinitesimal deformation of nuclei, described by parameter ε. To do so, we check for two conditions: (a) $\varepsilon = 0$ is an extremum of the energy density and (b) the extremum at $\varepsilon = 0$ is a (local) minimum. While conducting this analysis, we assume that the net baryon number density:

$$n_b = n_{ni}^{(\mathrm{tot})} + n_{pi}^{(\mathrm{tot})} + n_{no}^{(\mathrm{tot})} + n_{ns}^{(\mathrm{tot})} \tag{A23}$$

as well as nuclei number density n_N are constants, while the remaining (internal) CLDM parameters $n_{pi}^{(\mathrm{tot})}$, $n_{oi}^{(\mathrm{tot})}$, $n_{ns}^{(\mathrm{tot})}$ and u, generally, can vary with variations of ε.

As the first step, we need to specify equlibrium values of internal CLDM parameters, which are given by the condition that the partial derivatives with respect to each of internal parameters is zero. As long as we are interested in these parameters at $\varepsilon = 0$, i.e., for spherical nuclei, respective equations are exactly the same as in [26]. In particular, if n_N differs from the equilibrium value, Equation (4) holds true.

Let us note that the energy density explicitly depends only on ε^2, thus the partial derivative $\partial\epsilon/\partial\varepsilon \propto \varepsilon$, thus $\varepsilon = 0$ is indeed an extremum.

To check if the extremum at $\varepsilon = 0$ is minimum or maximum, we firstly note that the mixed partial derivatives $\partial^2\epsilon/\partial\varepsilon\partial p \propto \varepsilon$, and thus, they are zero, if calculated at $\varepsilon = 0$ (here, p is an arbitrary parameter of the CLDM model, except ε). As a result, the variation of energy density associated with infinitesimal ε is:

$$\delta\epsilon = \frac{1}{2}\frac{\partial^2\epsilon}{\partial\varepsilon^2}\bigg|_{\varepsilon=0}\varepsilon^2. \tag{A24}$$

The bulk terms in the energy density do not depend on ε explicitly and only the Coulomb and surface energy contributes to $\partial^2\epsilon/\partial\varepsilon^2$. These derivatives can be easily calculated (as long as ϵ depends on ε only via ε^2, $\partial^2\epsilon/\partial\varepsilon^2\big|_{\varepsilon=0} = 2\partial\epsilon/\partial\left(\varepsilon^2\right)\big|_{\varepsilon^2=0}$). While calculating the derivative of the surface energy, one should keep in mind that it is calculated at fixed $n_{ns}^{(\mathrm{tot})}$ and, thus, the fixed total amount of adsorbed neutrons. In this case, $\delta E_s = \sigma\delta\mathcal{A}$, due to Equation (A17), leading to:

$$\delta\epsilon = n_N\left[\frac{8\pi}{5}R^2\sigma + \frac{3}{5}\frac{Z^2e^2}{R}\left(\frac{u}{2} - \frac{1}{5}\right)\right]\varepsilon^2. \tag{A25}$$

Multiplying $\delta\epsilon$ to the cell volume V_c we arrive at Equation (1), which describes a change of the cell energy associated with nucleus deformation. Positiveness of this energy change guarantees stability with respect to infinitesimal deformations.

References

1. Haensel, P.; Potekhin, A.Y.; Yakovlev, D.G. *Neutron Stars 1: Equation of State and Structure*; Springer: New York, NY, USA, 2007; Volume 326, p. 620. [CrossRef]
2. Chamel, N.; Haensel, P. Physics of Neutron Star Crusts. *Living Rev. Rel.* **2008**, *11*, 10. [CrossRef] [PubMed]

3. Ravenhall, D.G.; Pethick, C.J.; Wilson, J.R. Structure of Matter below Nuclear Saturation Density. *Phys. Rev. Lett.* **1983**, *50*, 2066–2069. [CrossRef]
4. Hashimoto, M.; Seki, H.; Yamada, M. Shape of nuclei in the crust of a neutron star. *Prog. Theor. Phys.* **1984**, *71*, 320–326. [CrossRef]
5. Newton, W.G.; Gearheart, M.; Li, B.A. A Survey of the Parameter Space of the Compressible Liquid Drop Model as Applied to the Neutron Star Inner Crust. *Astrophys. J. Suppl. Ser.* **2012**, *204*, 9. [CrossRef]
6. Caplan, M.E.; Horowitz, C.J. Colloquium: Astromaterial science and nuclear pasta. *Rev. Mod. Phys.* **2017**, *89*, 041002. [CrossRef]
7. Dinh Thi, H.; Carreau, T.; Fantina, A.F.; Gulminelli, F. Uncertainties in the pasta-phase properties of catalysed neutron stars. *Astron. Astrophys.* **2021**, *654*, A114. [CrossRef]
8. Pearson, J.M.; Chamel, N.; Potekhin, A.Y. Unified equations of state for cold nonaccreting neutron stars with Brussels-Montreal functionals. II. Pasta phases in semiclassical approximation. *Phys. Rev. C* **2020**, *101*, 015802. [CrossRef]
9. Newton, W.G.; Kaltenborn, M.A.; Cantu, S.; Wang, S.; Stinson, A.; Rikovska Stone, J. Glassy quantum nuclear pasta in neutron star crusts. *arXiv* **2021**, arXiv:2104.11835.
10. Pearson, J.M.; Chamel, N. Unified equations of state for cold nonaccreting neutron stars with Brussels-Montreal functionals. III. Inclusion of microscopic corrections to pasta phases. *Phys. Rev. C* **2022**, *105*, 015803. [CrossRef]
11. Douchin, F.; Haensel, P. Inner edge of neutron-star crust with SLy effective nucleon-nucleon interactions. *Phys. Lett. B* **2000**, *485*, 107–114. [CrossRef]
12. Viñas, X.; Gonzalez-Boquera, C.; Sharma, B.K.; Centelles, M. Pasta-phase Transitions in the Inner Crust of Neutron Stars. *Acta Phys. Pol. B Proc. Suppl.* **2017**, *10*, 259. [CrossRef]
13. Pethick, C.J.; Ravenhall, D.G. Matter at Large Neutron Excess and the Physics of Neutron-Star Crusts. *Annu. Rev. Nucl. Part. Sci.* **1995**, *45*, 429–484. [CrossRef]
14. Iida, K.; Watanabe, G.; Sato, K. Formation of Nuclear "Pasta" in Cold Neutron Star Matter. *Prog. Theor. Phys. Suppl.* **2002**, *146*, 514–519. [CrossRef]
15. Bohr, N.; Wheeler, J.A. The Mechanism of Nuclear Fission. *Phys. Rev.* **1939**, *56*, 426–450. [CrossRef]
16. Chabanat, E.; Bonche, P.; Haensel, P.; Meyer, J.; Schaeffer, R. A Skyrme parametrization from subnuclear to neutron star densities. *Nucl. Phys. A* **1997**, *627*, 710–746. [CrossRef]
17. Chabanat, E.; Bonche, P.; Haensel, P.; Meyer, J.; Schaeffer, R. A Skyrme parametrization from subnuclear to neutron star densities Part II. Nuclei far from stabilities. *Nucl. Phys. A* **1998**, *635*, 231–256. [CrossRef]
18. Goriely, S.; Chamel, N.; Pearson, J.M. Further explorations of Skyrme-Hartree-Fock-Bogoliubov mass formulas. XIII. The 2012 atomic mass evaluation and the symmetry coefficient. *Phys. Rev. C* **2013**, *88*, 024308. [CrossRef]
19. Zemlyakov, N.A.; Chugunov, A.I.; Shchechilin, N.N. Non-spherical nucleon clusters in the mantle of a neutron star: CLDM based on Skyrme-type forces. *J. Phys. Conf. Ser.* **2021**, *2103*, 012004. [CrossRef]
20. Watanabe, G. Simulating Pasta Phases by Molecular Dynamics and Cold Atoms: Formation in Supernovae and Superfluid Neutrons in Neutron Stars. *Prog. Theor. Phys. Suppl.* **2010**, *186*, 45–50. [CrossRef]
21. Kubis, S.; Wójcik, W. The role of the electric Bond number in the stability of pasta phases. *arXiv* **2021**, arXiv:2102.06675.
22. Baym, G.; Bethe, H.A.; Pethick, C.J. Neutron star matter. *Nucl. Phys. A* **1971**, *175*, 225–271. [CrossRef]
23. Landau, L.D.; Lifshitz, E.M. *Statistical Physics*; Pergamon Press: Oxford, UK, 1980; Pt. 1–2.
24. Lattimer, J.M.; Pethick, C.J.; Ravenhall, D.G.; Lamb, D.Q. Physical properties of hot, dense matter: The general case. *Nucl. Phys. A* **1985**, *432*, 646–742. [CrossRef]
25. Brandt, S. *Kernestof under Nuklear Tæthed*; Niels Bohr Institute and Nordita, Copenhagen University: Copenhagen, Denmark, 1985.
26. Gusakov, M.E.; Chugunov, A.I. Thermodynamically Consistent Equation of State for an Accreted Neutron Star Crust. *Phys. Rev. Lett.* **2020**, *124*, 191101. [CrossRef]
27. Carreau, T.; Fantina, A.F.; Gulminelli, F. Inner crust of a neutron star at the point of crystallization in a multicomponent approach. *Astron. Astrophys.* **2020**, *640*, A77. [CrossRef]
28. Potekhin, A.Y.; Chabrier, G. Crust structure and thermal evolution of neutron stars in soft X-ray transients. *Astron. Astrophys.* **2021**, *645*, A102. [CrossRef]
29. Dinh Thi, H.; Fantina, A.F.; Gulminelli, F. The effect of the energy functional on the pasta-phase properties of catalysed neutron stars. *Eur. Phys. J. A* **2021**, *57*, 296. [CrossRef]